

# Magnetic Field Induced Dipolar Couplings in the Pretransitional Region of a Nematic Liquid Crystal

Denis Merlet,<sup>\*,†</sup> Anne Lesage,<sup>‡</sup> and James W. Emsley<sup>§</sup>

Laboratoire de Chimie Structurale Organique, ICMMO, ESA 8074, Bât. 410, Université de Paris-Sud, 91405 Orsay, France, Laboratoire de Chimie, Ecole Normale Supérieure de Lyon, 46 Allée d'Italie, 69364 Lyon Cedex 07, France, and School of Chemistry, University of Southampton, Southampton SO17 1BJ, United Kingdom

Received: February 7, 2005; In Final Form: April 15, 2005

<sup>13</sup>C and <sup>1</sup>H NMR spectroscopy have been used to study the orientational order which develops when a nematogenic compound, 4-pentyl-4'-cyanobiphenyl (5CB), approaches the transition from the isotropic to the nematic phase at  $T_{\text{NI}}$ . The experiments yield values of field induced dipolar couplings,  $^1D_{\text{CHi}}^{\text{B}}$ , between all of the directly bonded carbon and hydrogen nuclei in the molecule, and  $^2D_{\text{HH}}^{\text{B}}$ , the geminal dipolar coupling between protons in the first methylene group in the alkyl chain. The temperature dependence of these couplings shows that in each case they follow a divergence behavior governed by  $(T - T^*)^{-1}$ , where  $T^*$  is a temperature determined from the experimental data and which is close to but less than  $T_{\text{NI}}$ . Experiments performed at spectrometer field strengths of 11.75 and 18.79 T confirm the prediction that the induced couplings should depend on the square of the applied field strength. It was found that, within experimental error,  $T^*$  is the same for each field-induced coupling, and that  $T_{\text{NI}} - T^*$  is the same at 11.75 and 18.79 T. It is shown that the set of field-induced couplings  $^1D_{\text{CHi}}^{\text{B}}$  obtained at a temperature close to  $T_{\text{NI}}$  can be used to derive a conformer distribution for 5CB in the isotropic phase.

## Introduction

The molecules in all liquid crystalline phases have long-range orientational order which is dramatically reduced in magnitude on entering the isotropic phase at  $T_{\text{I}}$ , but which does not vanish entirely.<sup>1</sup> Some angular correlations between the molecules exist just above  $T_{\text{I}}$  which decrease rapidly with increasing temperature, defining the pre-transitional region, and are eventually lost. The extent of the pre-transitional ordering of the molecules can be demonstrated by measurement of anisotropic properties of the sample induced by the application of electric or magnetic fields. The measurement of optical properties of the sample, such as birefringence,  $\Delta n_{\text{ind}}$ , induced by electric or magnetic fields is the most sensitive way of revealing pre-transitional ordering, and they were the stimulus for developing theories for this phenomenon.<sup>2</sup> Thus, it was shown that values of  $\Delta n_{\text{ind}}$  depend on the square of the applied field and on  $(T - T^*)^{-1}$ , where  $T^*$  is identified by Landau–de Gennes theory as being the temperature at which a second-order transition to the liquid crystalline phase would occur if a first-order transition at  $T_{\text{I}}$  had not taken place. There is just one value of  $\Delta n_{\text{ind}}$  that can be measured for a particular liquid crystalline sample at each temperature, and so these experiments are not able to probe the effects of the molecular structure on the pre-transitional order. This became possible when it was shown that magnetic field induced quadrupolar splittings,  $\Delta\nu_i^{\text{B}}$ , of nuclei such as deuterium, can be observed by NMR spectroscopy when the static magnetic field,  $\mathbf{B}_0$ , is at least  $\sim 9$  T.<sup>3</sup> The first experiments were

on nonmesogenic compounds dissolved in isotropic solvents, but this stimulated work on deuterated mesogens<sup>4</sup> and dissolved solutes in mesogenic solvents<sup>5</sup> in the region close to  $T_{\text{NI}}$  where pre-transitional orientational order develops. However, there are some problems in realizing a wider application of deuterium NMR for studying pre-transitional order. The most important of these is that the spectral lines broaden as  $T_{\text{I}}$  is approached, which combined with the small chemical shift range for deuterium leads to strongly overlapping lines which are difficult to deconvolute. A second, general problem is that the spectrum does not yield the signs of the splittings and this leads to ambiguities in relating the magnitudes of the  $\Delta\nu_i^{\text{B}}$  to the molecular structure. The third disadvantage is that it has been necessary, so far, to enrich the molecules in deuterium to obtain spectra, although this may not be necessary with modern spectrometers in the future, particularly if deuterium cryoprobes are developed enabling <sup>2</sup>H spectra to be obtained at natural abundance.

We present here an alternative NMR method, which is to use <sup>13</sup>C and <sup>1</sup>H as the probe nuclei. Consider first the NMR spectrum of a single <sup>13</sup>C nucleus bonded to a group containing  $N_{\text{H}}$  equivalent protons. The spectrum at  $T \gg T_{\text{I}}$  will be dominated by the scalar coupling  $^1J_{\text{CH}}$  between the directly bonded carbon and hydrogen nuclei to produce a multiplet of  $N_{\text{H}} + 1$  lines. There may be further, smaller splittings from longer range couplings, which usually do not prevent a measurement of the magnitude of  $^1J_{\text{CH}}$ . On approaching  $T_{\text{I}}$ , the splittings will be modified to be

$$^1\Delta_{\text{CH}} = ^1J_{\text{CH}} + 2^1D_{\text{CH}}^{\text{B}} \quad (1)$$

where  $^1D_{\text{CH}}^{\text{B}}$  is a dipolar coupling induced by the magnetic field. The sign of  $^1J_{\text{CH}}$  can safely be taken to be positive, and

\* To whom correspondence should be addressed. E-mail: denismerlet@icmo.u-psud.fr.

<sup>†</sup> Université de Paris-Sud.

<sup>‡</sup> Ecole Normale Supérieure de Lyon.

<sup>§</sup> University of Southampton.

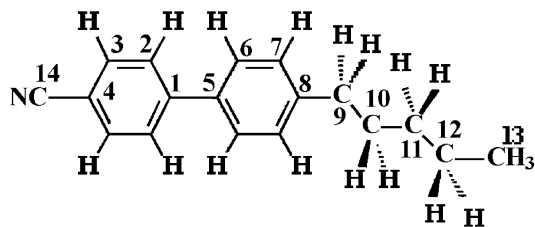


**Figure 1.** Structure and labeling of the nematogen 4-pentyl-4'-cyanobiphenyl (5CB).

there will always be temperatures when  $|^1J_{\text{CH}}| > |^1D_{\text{CH}}^{\text{B}}|$ , so that the magnitude of  $^1\Delta_{\text{CH}}$  provides both the magnitude and sign of  $^1D_{\text{CH}}^{\text{B}}$ . A second advantage is that  $^{13}\text{C}$  chemical shifts are large enough, particularly at high magnetic fields, that spectral overlap is considerably less of a problem than for deuterium, although not entirely absent. Finally, it is possible to obtain spectra with excellent signal-to-noise for natural abundance  $^{13}\text{C}$  so that tedious and costly isotope enrichment is not necessary. If longer-range couplings are resolved, either scalar or induced dipolar, these may complicate the spectrum but also yield more information.

Proton NMR spectra will also change for a liquid crystalline sample as  $T_{\text{i}}$  is approached from above. Induced dipolar couplings  $D_{\text{H,H}}^{\text{B}}$  will affect the spectra, but in a more complex way, which may require either more sophisticated experiments or second-order spectral analysis.

Field induced dipolar couplings can be observed in mesogenic samples at fields as low as 9.4 T, but as the couplings should depend on  $\mathbf{B}_0^2$  then there is an advantage in using a field as high as possible, provided that the line widths do not also increase with  $\mathbf{B}_0$ . Experiments are reported here on the nematogen 4-pentyl-4'-cyanobiphenyl (5CB), whose structure is shown in Figure 1, at field strengths of 9.4, 11.75, and 18.79 T, which enabled the effect of field strength on the spectra to be investigated. The main objectives of this paper are to demonstrate that the induced couplings obtained can be used to test the molecular mean field theory of pre-transitional ordering, principally via the form of the temperature dependence of  $D_{ij}^{\text{B}}$ , and also to show how they may be used to determine the orientational order and conformational distribution of the molecules in the pre-transitional region.

## Experimental Section

**NMR Spectroscopy.** A sample of pure 5CB was obtained from Merck. It had a nematic–isotropic transition temperature of  $T_{\text{NI}} = 308.4$  K. The different spectra were recorded at the three field strengths. The three spectrometers used were a Bruker DRX 400 MHz, a Varian Unity + 500 MHz, and a Varian Inova 800 MHz. In each case, the temperature was controlled by the standard equipment supplied by the spectrometer manufacturers. These have a setting precision of 0.1 °C. A temperature gradient over the probe coil volume will produce a broadening of the spectral lines, and the observed line widths and shapes suggest that the gradients for each of the three spectrometers used was  $< 0.05$  °C.

The proton spectra were obtained with 8 acquisitions on 16 384 points, and 64 for the carbon-13 spectra on 16 384 points. Proton irradiation was not used during the acquisition period, because the  $^{13}\text{C}$ – $^1\text{H}$  couplings are required. Irradiating the protons between acquisitions is usually used even when not used for decoupling, to improve the signal strength by the NOE effect. This was not done here since it can lead to an unacceptable amount of sample heating.

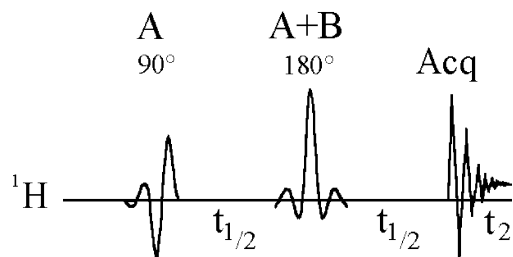


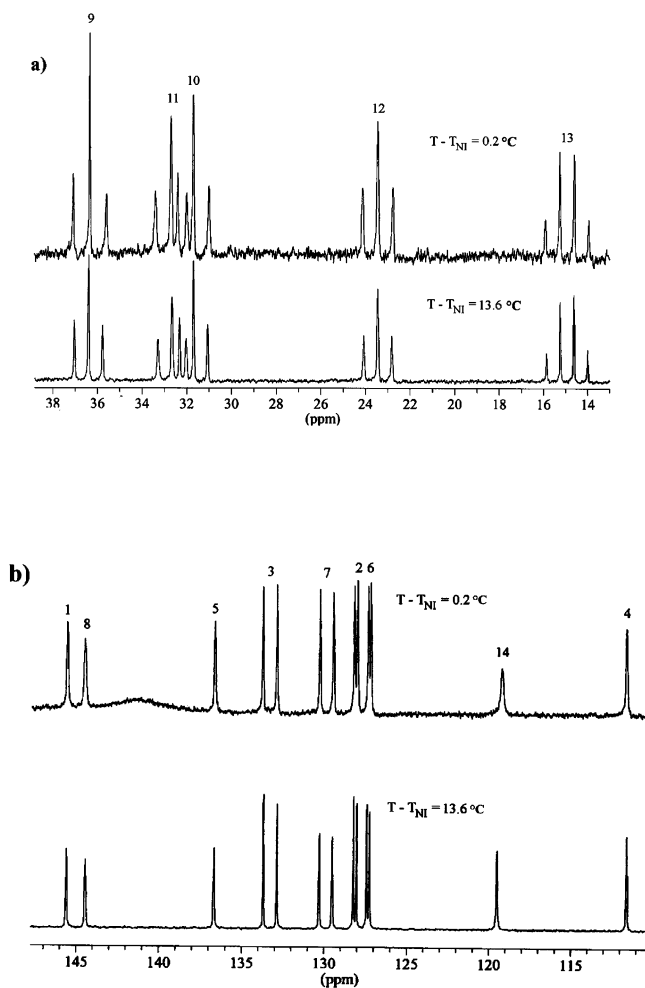
**Figure 2.** Pulse sequence for the selective refocusing experiment (SERF). The first pulse is a 90° pulse selective to resonance A, which is coupled to B. The second pulse is a 180° pulse applied to both A and B resonances.

At temperatures more than 2 °C above  $T_{\text{NI}}$ , the  $^{13}\text{C}$  lines show evidence of long-range coupling, but this becomes unresolved at lower temperatures, and a Lorentzian line broadening of 2 Hz was applied to increase the signal-to-noise ratio. Zero-filling of the  $^{13}\text{C}$  fids to 128 k was applied to increase the digital resolution. Two-dimensional (2D) selective refocusing (SERF) spectra<sup>6</sup> were obtained using the pulse sequence shown in Figure 2. The 2D SERF experiment was applied to the protons of the methylene group attached to the phenyl ring (note that in this case, both selective pulses are applied to the A and B proton spins since the two methylene protons have degenerate chemical shifts). E-BURP2 and RE-BURP shaped pulses were used as selective excitation and refocusing pulses, respectively.<sup>7</sup> The length of the two selective pulses was 14.5 ms. Spectral widths of 30, 40, and 150 Hz in F1 were used for spectra recorded at 9.4, 11.75, and 18.79 T, respectively. A total of 64  $t_1$  points were recorded with 8 scans each. A square cosine apodization was applied in both dimensions.

**Measurement of the Field-Induced Splittings.** The  $^1\text{H}$  and  $^{13}\text{C}$  spectra were assigned by a standard 2D HSQC experiment and a 2D INADEQUATE experiment<sup>8</sup> recorded at 9.4 T on a sample of pure 5CB in the isotropic phase at 323.0 K (not shown). Having assigned the spectral lines, the next step was to record a  $^{13}\text{C}$  spectrum at 9.4 T of a sample dissolved in  $\text{CDCl}_3$  to obtain the  $^1\text{H}$ – $^{13}\text{C}$  scalar coupling.  $^1\text{H}$  and  $^{13}\text{C}$  spectra were then recorded for pure 5CB at the three field strengths and over a range of temperatures in the isotropic phase. Figure 3 shows the carbon spectra of 5CB taken at  $T - T_{\text{NI}}$  of 0.2 and 13.6 °C at 18.79 T. The carbon spectra are simple to analyze, and values of  $^1\Delta_{\text{CH}}$  are obtained from peak separations by fitting line shapes.

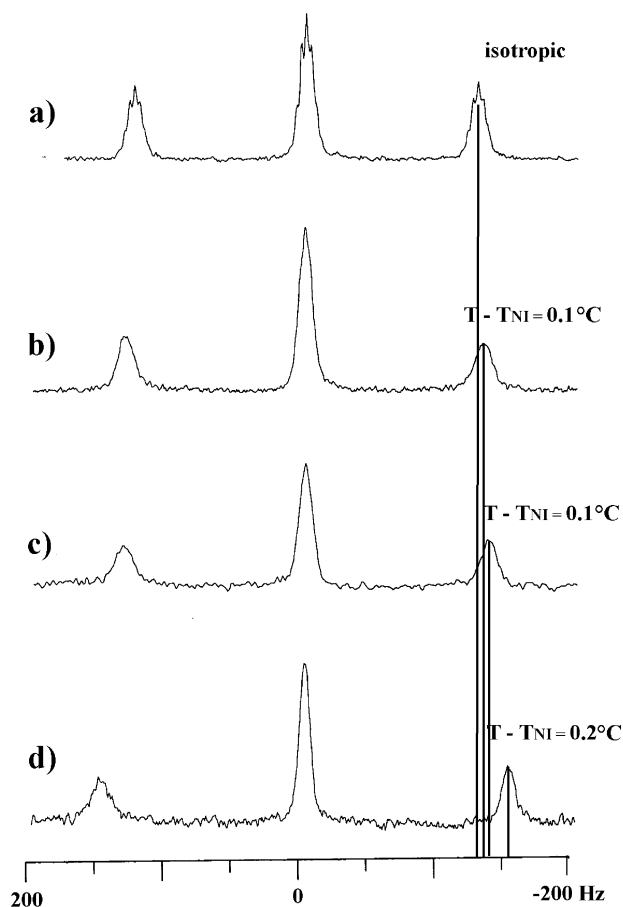
Figure 4 shows the triplet from the carbon at position 9 at the three field strengths, and also for the sample dissolved in  $\text{CDCl}_3$ . Note that the line widths in the  $^{13}\text{C}$  spectra of pure 5CB are broader than those for the  $\text{CDCl}_3$  solution and they increase as  $T_{\text{NI}}$  is approached. They do not, however, depend on the magnetic field strength. The splittings  $^1\Delta_{\text{CH}_i}$  obtained at  $\mathbf{B}_0$  values of 11.75 and 18.79 T are given in Tables 1 and 2, respectively; the values measured at 9.4 T are not given: they are small, and obtained with poor precision.

Figure 5 shows the  $^1\text{H}$  spectra of 5CB at 18.79 T at  $T - T_{\text{NI}}$  of 0.2 and 13.6 °C. The broadening of the lines as  $T_{\text{NI}}$  is approached is more important for proton than carbon spectra because it leads to a loss of spectral resolution making it difficult, if not impossible, to extract values of  $D_{ij}^{\text{B}}$  for most sites in the molecule. There may also be an increase in complexity of the multiplet pattern of the  $\text{CH}_2$  groups as the induced dipolar couplings increase in magnitude. This is clearly seen for the methylene group at position 9 (resonance at 2.6 ppm). At  $T - T_{\text{NI}} = 13.6$  °C the spectrum is a triplet, which is an example of “deceptive simplicity”. These methylene protons



**Figure 3.** (a) Aliphatic part, and (b) aromatic part of 200 MHz  $^{13}\text{C}$  spectra ( $B_0 = 18.79$  T) of 5CB at  $T - T_{\text{NI}}$  of 0.2 and 13.6 °C.

are not magnetically equivalent and to describe correctly the spectrum it is sufficient to consider them as the  $AA'$  part of an  $AA'MM'$  spin system, if we consider coupling to only the  $\beta$  methylene group. The spectra depend on the coupling constants  ${}^3J_{AM} = {}^3J_{A'M'}$ ,  ${}^4J_{AM'} = {}^4J_{A'M}$ ,  ${}^3J_{AA'}$ , and  ${}^3J_{MM'}$ , and the  $AA'$  and  $MM'$  parts should each consist of 10 lines. However, the spectrum of the methylene protons at the position 9 appears as a simple 1:2:1 triplet because of a particular combination of the values of the coupling constants and chemical shifts. When the induced dipolar couplings become appreciable compared with the scalar couplings, then the total couplings may no longer be such as to produce deceptive simplicity, and a more complex multiplet results. This is clearly seen in Figure 5 for the methylene group at position 9, which evolves from a triplet into an ill-resolved doublet-like structure. One way of changing the spin system for such a methylene group is to do a 2D selective spin-echo experiment (SERF).<sup>6</sup> When all selective pulses are applied on the methylene protons, the spin-echo sequence refocuses the chemical shifts and all couplings to nonresonant spins, and converts the spin system to an oriented  $A_2$  spin system, which gives a doublet with separation  $3D_{AA'}$ . The result of such a SERF experiment done at 800 MHz on the  $\text{C}_9$  methylene protons is shown in Figure 6, where it is seen that the projection on the F1 axis is indeed a doublet; the small central peak arises from imperfections in the RF pulses. The SERF experiment allowed the temperature dependence of  $D_{\text{HH}9}^{\text{B}}$  to be obtained, as shown in Figure 7.



**Figure 4.**  $^{13}\text{C}$  spectra of the carbon 9 of 5CB for a sample (a) dissolved in  $\text{CDCl}_3$  at 9.4 T, for pure sample in the isotropic phase close to  $T_{\text{NI}}$  at field strengths of (b) 9.4, (c) 11.75, and (d) 18.79 T. The vertical lines illustrate how the splitting increases with increasing the field. A Lorentzian line broadening of 1 Hz was applied to increase the signal-to-noise ratio.

**TABLE 1: Splittings  ${}^1\Delta_{\text{CH}i}$  (in Hz) Obtained at a  $B_0$  Value of 11.75 T for Different Shifted Temperatures  $T - T_{\text{NI}}$  in °C<sup>a</sup>**

$i$	2	3	6	7	9	10	11	12	13
$T - T_{\text{NI}}$									
7.1	162.1	165.7	156.9	156.8	126.8	125.2	123.7	125.7	124.8
5.1	162.2	165.8	157.0	156.9	127.6	125.4	123.8	126.2	125.0
3.1	162.4	166.0	157.0	156.9	128.0	125.7	124.4	126.2	125.2
2.9	162.4	166.0	157.1	157.0	128.4	125.7	123.9	126.4	125.1
2.7	162.4	165.9	157.1	156.9	128.1	126.0	124.2	126.6	125.1
2.5	162.4	166.0	157.1	157.1	128.1	125.9	124.0	126.5	125.0
2.3	162.5	166.0	157.2	157.1	128.2	125.9	125.1	126.4	125.4
2.1	162.5	166.1	157.2	157.1	128.7	126.2	124.8	126.6	125.3
1.9	162.6	166.2	157.2	157.1	128.7	126.3	125.4	126.7	125.3
1.7	162.6	166.1	157.2	157.1	128.6	126.4	124.8	126.9	125.3
1.5	162.7	166.2	157.3	157.2	129.3	126.3	124.6	126.7	125.4
1.3	162.8	166.4	157.3	157.3	129.6	126.9	125.9	126.8	125.8
1.1	163.0	166.4	157.3	157.3	129.9	127.2	125.8	127.1	126.1
0.9	163.2	166.5	157.4	157.5	130.2	127.3	125.8	127.1	126.1
0.7	163.2	166.7	157.4	157.5	131.3	127.5	126.3	128.0	126.3
0.5	163.6	166.9	157.6	157.6	132.3	128.2	126.3	128.0	126.4
0.3	164.0	167.2	157.9	158.0	133.8	128.8	127.4	128.8	126.8
0.1	164.5	167.7	158.3	158.2	135.5	130.3	128.6	129.2	127.4

<sup>a</sup> The letter  $i$  refers to the carbon position according to the labelling of Figure 1.

## Results and Discussion

The molecules of 5CB are flexible by virtue of rotations about bonds, and they can be considered to exist in a set of rigid conformations. A biaxial molecule in the  $n$ th conformation in

**TABLE 2: Splittings  $^1\Delta_{\text{CH}_i}$  (in Hz) Obtained at  $B_0$  Value of 18.79 T for Different Shifted Temperatures  $T - T_{\text{NI}}$  in  $^{\circ}\text{C}^a$** 

$i$	2	3	6	7	9	10	11	12	13
$T - T_{\text{NI}}$									
13.6	162.3	165.7	157.0	157.2	127.4	127.0	125.7	126.2	124.9
11.6	162.3	165.8	157.3	157.3	127.7	126.9	126.1	126.3	125.0
9.6	162.3	165.8	157.3	157.4	128.2	127.1	126.5	126.6	125.1
7.6	162.5	165.9	157.4	157.4	128.6	127.4	126.6	126.7	125.3
5.6	162.7	166.1	157.5	157.6	129.4	127.9	127.1	126.9	125.5
4.6	162.9	166.2	157.8	157.6	129.8	128.2	127.8	127.1	125.7
3.6	163.1	166.3	157.7	157.8	130.7	128.8	128.5	127.6	126.1
3.1	163.2	166.5	157.9	158.0	131.2	129.1	128.5	127.6	126.4
2.6	163.5	166.7	158.1	158.2	132.2	129.5	129.1	128.1	126.4
2.4	163.6	166.8	158.2	158.2	132.5	129.8	129.2	128.4	126.7
2.2	163.6	167.0	158.3	158.3	133.0	129.9	129.7	128.5	126.7
2.0	163.9	167.0	158.5	158.4	133.4	130.6	129.8	128.5	126.7
1.8	163.9	167.2	158.6	158.5	133.9	130.6	130.2	129.0	127.0
1.6	164.2	167.3	158.7	158.7	134.6	131.0	130.6	129.2	127.3
1.4	164.4	167.6	158.9	158.9	135.2	131.6	131.5	129.5	127.4
1.2	164.7	167.8	159.2	159.1	136.2	132.1	132.0	129.8	127.8
1.0	165.1	168.0	159.4	159.4	137.6	132.9	133.0	130.4	128.1
0.8	165.6	168.5	159.8	159.7	139.4	134.0	134.1	131.1	128.7
0.6	166.1	169.1	160.4	160.3	141.6	135.6	135.9	132.1	129.3
0.4	167.2	170.0	161.2	161.0	145.7	137.8	138.8	133.7	130.6
0.2	168.3	171.2	162.1	161.9	149.9	140.9	140.9	135.4	131.8

<sup>a</sup> The letter  $i$  refers to the carbon position according to the labelling of Figure 1.

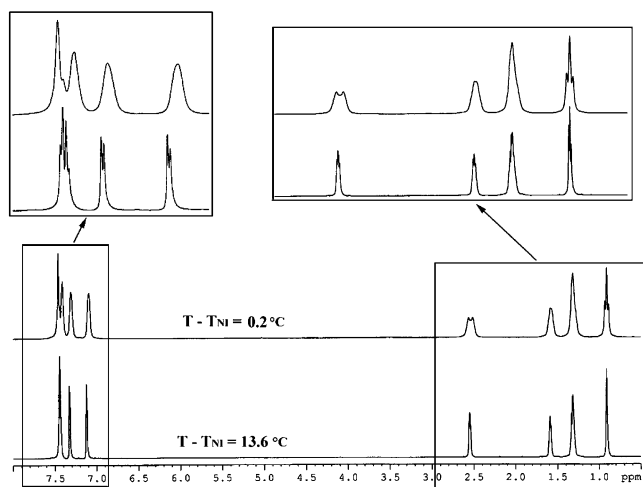


**Figure 5.** 800 MHz  $^1\text{H}$  spectra ( $B_0 = 18.79$  T) of 5CB at  $T - T_{\text{NI}}$  of 0.2 and 13.6  $^{\circ}\text{C}$ .

the presence of  $B_0$ , the magnetic field of the NMR spectrometer, will experience a magnetic torque given by<sup>1,9,10</sup>

$$U_{\text{mag}}^n(\beta_n, \gamma_n, n) = -(1/2)B_0^2[\chi_{2,0}^n C_{2,0}(\beta_n) + 2\chi_{2,2}^n C_{2,2}(\beta_n, \gamma_n)] \quad (2)$$

where the  $\chi_{2,m}^n$  are components of the anisotropic part of the molecular magnetic susceptibility tensor in irreducible form, and the  $C_{2,m}(\beta_n, \gamma_n)$  are second-rank, modified spherical harmonics;<sup>11</sup>  $\beta_n$  and  $\gamma_n$  are polar angles made by  $B_0$  in the principal frame of the tensor  $\chi^n$ .

The molecules also interact with each other such that, by analogy with molecules in liquid crystalline phases, a local director can be defined, and the anisotropic potential of a molecule in the average field of all its neighbors is

$$U_{\text{mol}}^n(\beta_n, \gamma_n, n) = - \sum_{L,m}^{\infty} \epsilon_{L,m}^n C_{L,m}(\beta_n, \gamma_n) \quad (3)$$

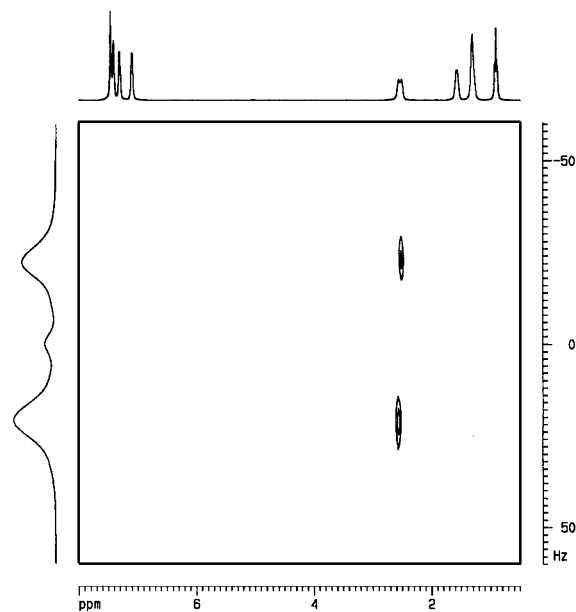


**Figure 6.** 800 MHz  $^1\text{H}$  SERF spectrum of 5CB at  $T - T_{\text{NI}} = 0.2$   $^{\circ}\text{C}$ .

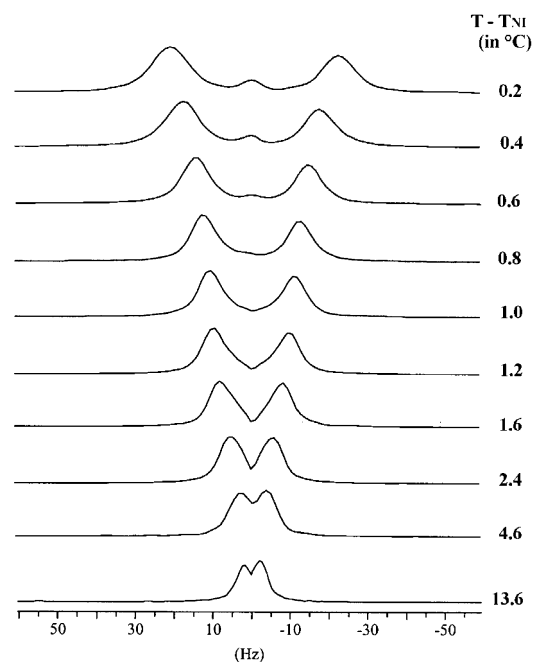


**Figure 7.** Projection on F1 of the 2D SERF spectrum at various values of  $T - T_{\text{NI}}$  at 18.79 T.

where the expansion coefficients  $\epsilon_{L,m}^n$  describe the strength of the anisotropic intermolecular potential.

The infinite expansion is approximated by restricting the summation to terms with  $L = 2$  to give

$$U_{\text{mol}}^n(\beta_n, \gamma_n, n) = -\epsilon_{2,0}^n C_{2,0}(\beta_n) - 2\epsilon_{2,2}^n C_{2,2}(\beta_n, \gamma_n) \quad (4)$$

where it has been assumed that the principal axes for the interaction tensor  $\epsilon^n$  are collinear with those of  $\chi^n$ . Note that the second term on the right-hand side of eq 4 is nonzero only for biaxial molecules. For a molecule with a positive anisotropy of the diamagnetic susceptibility, the local directors are aligned along  $B_0$ . In this case the total anisotropic mean energy,  $U_{\text{sum}}^n(\beta_n, \gamma_n, n)$ , is



$$\begin{aligned}
U_{\text{sum}}^n(\beta_n, \gamma_n, n) &= U_{\text{mol}}^n(\beta_n, \gamma_n, n) + U_{\text{mag}}^n(\beta_n, \gamma_n, n) \\
&= -\{\epsilon_{2,0}^n + (1/2)\mathbf{B}_0^2 \chi_{2,0}^n\} C_{2,0}(\beta_n) - \{2\epsilon_{2,2}^n + \mathbf{B}_0^2 \chi_{2,2}^n\} C_{2,2}(\beta_n, \gamma_n) \\
&= -X_{2,0}^n C_{2,0}(\beta_n) - 2X_{2,2}^n C_{2,2}(\beta_n, \gamma_n) \quad (5)
\end{aligned}$$

The molecules will have a degree of orientational order relative to the magnetic field direction, and for second-rank interactions such as the dipolar coupling, only the second-rank order parameters,  $\bar{C}_{2,m}^n$ , are required, and these are given by

$$\bar{C}_{2,m}^n = (1/4\pi) \int_0^{2\pi} d\gamma_n \int_0^\pi \sin \beta_n d\beta_n [C_{2,m}^n \exp\{-U_{\text{sum}}^n(\beta_n, \gamma_n, n)/k_B T\}] \quad (6)$$

In the isotropic phase  $U_{\text{sum}}^n(\beta_n, \gamma_n, n)/k_B T \ll 1$  so that the exponential may be truncated to  $\{1 - U_{\text{sum}}^n(\beta_n, \gamma_n, n)/k_B T\}$ , and the orthogonality of the  $C_{2,m}(\beta_n, \gamma_n)$  leads to the simple result

$$\bar{C}_{2,m}^n = X_{2,m}^n / (5k_B T) \quad (7)$$

Note that this simple result means that eq 3 can be regarded as being exact rather than an approximation.

When  $T \gg T_{\text{NI}}$ ,  $\epsilon_{2,m}^n \ll \mathbf{B}_0^2 \chi_{2,m}^n$  and  $X_{2,m}^n = (1/2)\mathbf{B}_0^2 \chi_{2,m}^n$ , and the induced ordering is that for a single molecule. When  $T$  is close to  $T_{\text{NI}}$ , the condition  $\epsilon_{2,m}^n \gg \mathbf{B}_0^2 \chi_{2,m}^n$  is approached, and now the conformational order parameters  $\bar{C}_{2,m}^n$  are dominated by the magnitude of the anisotropic, intermolecular interactions.

**Temperature Dependence of the Induced Dipolar Splittings.** To understand the temperature dependence of the induced ordering, and hence of the dipolar couplings, it is necessary to propose a relationship between the interaction coefficients,  $\epsilon_{2,m}^n$ , and the order parameters,  $\bar{C}_{2,m}^n$ . The coefficients must vanish when the orientational order vanishes, and so the simplest form for this relationship is<sup>1,9</sup>

$$\epsilon_{2,0}^n = u_{200}^n \bar{C}_{2,0}^n + u_{202}^n \bar{C}_{2,2}^n \quad (8)$$

$$\epsilon_{2,2}^n = u_{220}^n \bar{C}_{2,0}^n + u_{222}^n \bar{C}_{2,2}^n \quad (9)$$

The coefficients  $u_{2mn}$  depend on the nature of the anisotropic intermolecular forces.<sup>10</sup> We will also invoke the standard approximations of the molecular mean field theory

$$u_{202}^n = u_{220}^n = (u_{200}^n u_{222}^n)^{1/2} \quad (10)$$

which together with eq 7 leads to the relationships<sup>9</sup>

$$\bar{C}_{2,0}^n = \frac{[\lambda_n u_{200}^n (\chi_{2,2}^n - \lambda_n \chi_{2,0}^n) + 5k_B T \chi_{2,0}^n] \mathbf{B}_0^2}{50k_B^2 T (T - T^{n*})} \quad (11)$$

$$\bar{C}_{2,2}^n = \frac{[u_{200}^n (\lambda_n \chi_{2,0}^n - \chi_{2,2}^n) + 5k_B \lambda_{2,2}^n T] \mathbf{B}_0^2}{50k_B^2 T (T - T^{n*})} \quad (12)$$

where  $T^{n*}$  is

$$T^{n*} = u_{200}^n (1 + \lambda_n^2) / 5k_B \quad (13)$$

and is the temperature at which a second-order transition to the nematic phase would occur if the first-order transition at  $T_{\text{NI}}$  had not taken place, where

$$\lambda_n = u_{220}^n / u_{200}^n \quad (14)$$

The induced dipolar coupling  $D_{ij}^{nB}(T)$  between nuclei  $i$  and  $j$  in conformation  $n$  at temperature  $T$  is given by

$$D_{ij}^{nB}(T) = -K_{ij} \bar{C}_{ij}^n / \langle r_{ijn}^3 \rangle \quad (15)$$

where  $\bar{C}_{ij}^n$  is an order parameter for the direction along the vector  $\mathbf{r}_{ijn}$ , and  $\langle r_{ijn}^3 \rangle$  is an average over small-amplitude vibrational motion. The constant  $K_{ij}$  is

$$K_{ij}/\text{Hz} = \mu_0 \gamma_i \gamma_j \hbar / 16\pi^3 \quad (16)$$

and is independent of  $n$ .

Transforming to the principal axis frame for the order matrix  $\bar{C}^n$  gives

$$D_{ij}^{nB}(T) = -(K_{ij} / \langle r_{ijn}^3 \rangle) [\bar{C}_{2,0}^n (3 \cos^2 \theta_{ijn} - 1) / 2 + ((3/2))^{1/2} \bar{C}_{2,2}^{n*} \sin^2 \theta_{ijn} \cos 2\phi_{ijn}] \quad (17)$$

The angles  $\theta_{ijn}$  and  $\phi_{ijn}$  describe the orientation of  $\mathbf{r}_{ijn}$  in the principal frame of the molecular order tensor.

The observed induced dipolar couplings are averages over all of the conformations

$$D_{ij}^B(T) = \sum_n P(n, T) D_{ij}^{nB}(T) \quad (18)$$

The probability,  $P(n, T)$  that the molecule has conformation  $n$  at temperature  $T$  is given by

$$P(n, T) = Q^{-1} \int \exp[-U_{\text{total}}^n(\beta_n, \gamma_n, n)/k_B T] \sin \beta_n d\beta_n d\gamma_n \quad (19)$$

with

$$Q = \sum_n \int \exp[-U_{\text{total}}^n(\beta_n, \gamma_n, n)/k_B T] \sin \beta_n d\beta_n d\gamma_n \quad (20)$$

$U_{\text{total}}^n(\beta_n, \gamma_n, n)$ , the total mean potential for conformer  $n$ , is the anisotropic potential  $U_{\text{sum}}^n(\beta_n, \gamma_n, n)$  plus  $U_{\text{int}}(n)$ , the energy of the conformer which is independent of orientation, and which is determined by the bond rotation potentials. Thus

$$U_{\text{total}}^n(\beta_n, \gamma_n, n) = U_{\text{sum}}^n(\beta_n, \gamma_n, n) + U_{\text{int}}(n) \quad (21)$$

The temperature dependence of  $D_{ij}^B(T)$  can be obtained by using eqs 10–18, but it is more useful to consider first how the complex expressions involved may simplify. The complexity stems from allowing for the biaxiality in the ordering of the individual conformers. If the biaxiality can be neglected, then the simple result is obtained

$$D_{ij}^B(T) = \frac{A_{ij} \{\chi_{2,0}^n, P_2(\cos \theta_{ij}^n)\} \mathbf{B}_0^2}{T - T^*} \quad (22)$$

with

$$T^* = \sum_n P(n, T = T^*) u_{200}^n / 5k_B \quad (23)$$

The proportionality constant  $A_{ij} \{\chi_{2,0}^n, P_2(\cos \theta_{ij}^n)\}$  is an average over all conformations, and depends on  $i$  and  $j$ , but  $T^*$  is the same for all couplings. Note that all of the couplings are directly proportional to  $\mathbf{B}_0^2$ . The effect of biaxial ordering is in principle to produce deviations from the behavior predicted by eq 22,

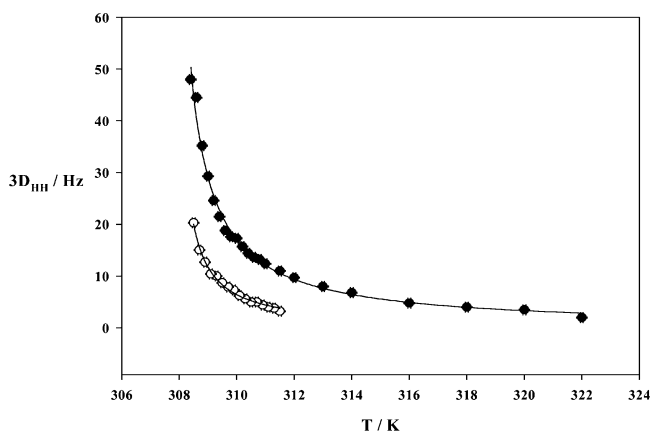


**Figure 8.** Temperature dependence of  $3D_{\text{HH}}^{\text{B}}$ , the peak separation measured by the SERF experiment for the methylene protons at position 9 in the alkyl chain in 5CB. The points (●) are for  $\mathbf{B}_0 = 18.79$  T, and the (○) are for  $\mathbf{B}_0 = 11.75$  T. The curves are best least-squares fits to eq 24.

**TABLE 3: Values of  $a_{\text{HH}}$  and  $T^*$  Obtained by Fitting  $3D_{\text{HH}}^{\text{B}}$  to eq 24 at Field Strengths of 11.79 and 18.89 T**

$\mathbf{B}_0/\text{T}$	11.79	18.89
$a_{\text{HH}}/\text{Hz K}^{-1}$	$14.2 \pm 0.4$	$41.4 \pm 1.4$
$T^*/\text{K}$	$307.79 \pm 0.03$	$307.58 \pm 0.04$

with a more complex dependence on temperature, but retaining the dependence of all of the  $D_{ij}^{\text{B}}$  on  $\mathbf{B}_0^2$ .

Figure 8 shows the temperature dependence of  $3D_{\text{HH}}$ , the splitting determined from the SERF experiments for the pair of methylene protons at the  $\alpha$  chain position. The values obtained for  $a_{\text{HH}}$  and  $T^*$  by fitting the data for  $3D_{\text{HH}}^{\text{B}}$  to eq 24 are given in Table 3.

$$3D_{\text{HH}} = a_{\text{HH}}/(T - T^*) \quad (24)$$

The values of  $a_{\text{HH}}$  are predicted to be dependent on  $\mathbf{B}_0^2$ , and their observed ratio of  $2.9 \pm 0.2$  is in good agreement with the expected value of 2.6.

The splittings  ${}^1\Delta_{\text{C,H}}$  measured from the  ${}^{13}\text{C}$  spectra all follow the relationship

$${}^1\Delta_{\text{C,H}} = a_i/(T - b_i) + c_i \quad (25)$$

to good precision, as illustrated in Figure 9 for the  $\text{C}_9\text{-H}$  splitting.

The values obtained for  $a_i$ ,  $b_i$ , and  $c_i$  are given in Table 4. Figure 10 shows the ratio  $a_i(18.79 \text{ T})/a_i(11.75 \text{ T})$  for both HH and C-H data. The slope of the plot in Figure 10 is  $2.9 \pm 0.1$ , with an intercept of  $-0.3 \pm 0.6$ , which compares with the expected values of 2.6 and 0. The mean values of  $T_{\text{NI}} - T^*$  are  $0.63 \pm 0.01$  °C for the data obtained at  $\mathbf{B}_0 = 11.75$  T, and  $0.6 \pm 0.1$  °C for 18.79 T, and there is no evidence, therefore, for a dependence of  $T_{\text{NI}} - T^*$  on the magnetic field strength. The values found here are significantly smaller than that of  $0.9$  °C obtained from field-induced deuterium quadrupolar splittings at 9.4 T,<sup>4</sup> and from Kerr constant measurements, using a DC electric field, of  $1.1 \pm 0.3$  °C.<sup>12</sup> Note that the values of  $c_i$  are in all cases within experimental error equal to  ${}^1J_{\text{CH}_i}$  measured for the isotropic solution in  $\text{CDCl}_3$ .

**Structure and Conformation from Induced Couplings.** It is possible to use values of  $D_{ij}^{\text{B}}(T)$  to determine the conformational distribution and orientational order of the molecules in the pre-transitional region in a manner analogous to that used for molecules in the liquid crystalline phase. Thus, as the

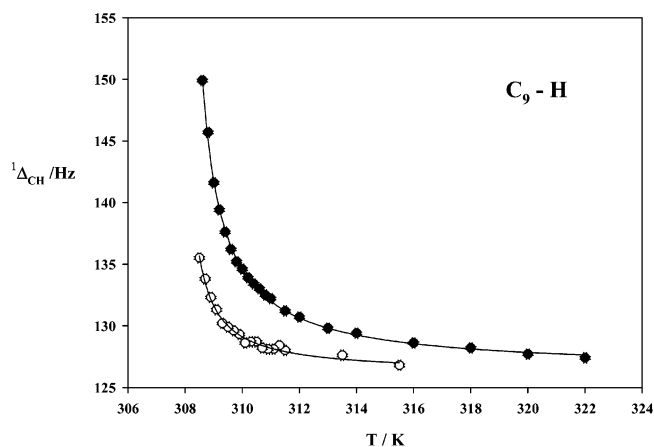


**Figure 9.** Temperature dependence of the induced splitting  ${}^1\Delta_{\text{C,H}}$  for the  $\text{C}_9$  position, at 11.75 T (open) and 18.79 T (closed symbols). The curves are best fits to eq 25.

temperature approaches  $T_{\text{NI}}$ , the mean anisotropic potential given by eq 5 becomes dominated by  $U_{\text{mol}}^n(\beta_n, \gamma_n, n)$ . This has the same form as that used to describe the mean anisotropic potential for a molecule in the nematic phase, except that now the truncation of the infinite expansion of eq 3 at the terms with  $L = 2$  can be regarded as being exact, rather than an approximation.  $U_{\text{total}}^n(\beta_n, \gamma_n, n)$  becomes

$$U_{\text{total}}^n(\beta_n, \gamma_n, n) = U_{\text{mol}}^n(\beta_n, \gamma_n, n) + U_{\text{int}}(n) \quad (26)$$

When the mean potential is expressed in this way, it is possible to obtain the conformational distribution  $P(n, T)$  by fitting observed to calculated data, but it is also possible to determine  $P_{\text{iso}}(n, T)$ , which is defined as

$$P_{\text{iso}}(n, T) = Q_{\text{iso}}^{-1} \exp[-U_{\text{int}}(n)/k_{\text{B}}T] \quad (27)$$

with

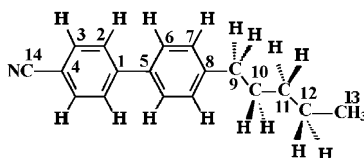
$$Q_{\text{iso}} = \sum_n \exp[-U_{\text{int}}(n)/k_{\text{B}}T] \quad (28)$$

$P_{\text{iso}}(n, T)$  is the conformational distribution for an isotropic distribution of the molecules at temperature  $T$ . For 5CB in the nematic phase,  $P(n, T)$  and  $P_{\text{iso}}(n, T)$  are substantially different.<sup>13,14</sup> Thus,  $P(\text{ttt}, T = 286 \text{ K})$ , the probability of the conformer with a fully extended chain was determined to be 0.42 (normalized over 27 chain conformations), whereas the value determined for  $P_{\text{iso}}(\text{ttt}, T = 286 \text{ K})$  was predicted to be 0.31, a reduction by a factor of 0.75. The interesting question arises as to whether  $P(n, T)$  obtained for the molecules in the isotropic phase from the data sets  $D_{ij}^{\text{B}}(T)$  will be equal to  $P_{\text{iso}}(n, T)$  obtained from the nematic phase data, making allowance for the difference in temperature.

The conformational probabilities for the pre-transitional region will be derived from the values of  $D_{ij}^{\text{B}}(T)$  in the same way as was done for the nematic phase data, using the same theoretical model and the same molecular geometry. Thus, the additive potential (AP) model is used for the conformational dependence of the interaction coefficients  $\epsilon_{2,m}^n$  in eq 2 to give

$$\epsilon_{2,m}^n = \sum_n \epsilon_{2,p}(j) D_{p,m}^2(\Omega_j^n) \quad (29)$$

where  $\epsilon_{2,p}(j)$  is a contribution to  $\epsilon_{2,m}^n$  from the  $j$ th rigid, molecular fragment, whose orientation to a molecular reference

**TABLE 4:** Values of  $a_i$ ,  $b_i$ , and  $c_i$  Obtained by Fitting  ${}^1\Delta_{\text{CH}}$  Splittings to eq 24 for Spectra Obtained at 11.75 and 18.79 T<sup>a</sup>

carbon, $i$	$B_0/T$	$a_i/(\text{Hz K}^{-1})$	$b_i/\text{K}$	$c_i/\text{Hz}$	${}^1J_{\text{CH}_i}/\text{Hz}$ (all $\pm 0.4$ )
2	11.8	$1.9 \pm 0.1$	$307.79 \pm 0.05$	$161.83 \pm 0.05$	162.1
	18.8	$5.1 \pm 0.2$	$307.82 \pm 0.02$	$161.87 \pm 0.04$	
3	11.8	$1.5 \pm 0.1$	$307.82 \pm 0.06$	$165.53 \pm 0.04$	165.5
	18.8	$4.0 \pm 0.1$	$307.91 \pm 0.02$	$165.42 \pm 0.03$	
6	11.8	$0.64 \pm 0.08$	$308.85 \pm 0.05$	$156.89 \pm 0.03$	156.9
	18.8	$4.1 \pm 0.2$	$307.83 \pm 0.03$	$156.85 \pm 0.05$	
7	11.8	$1.2 \pm 0.2$	$307.7 \pm 0.1$	$156.64 \pm 0.06$	156.7
	18.8	$3.8 \pm 0.1$	$307.84 \pm 0.02$	$156.94 \pm 0.03$	
9	11.8	$6.4 \pm 0.6$	$307.83 \pm 0.06$	$126.2 \pm 0.2$	126.2
	18.8	$17.55 \pm 0.05$	$307.86 \pm 0.02$	$126.18 \pm 0.06$	
10	11.8	$3.7 \pm 0.4$	$307.82 \pm 0.06$	$124.7 \pm 0.1$	125.5
	18.8	$10.2 \pm 0.2$	$307.91 \pm 0.02$	$126.18 \pm 0.06$	
11	11.8	$4.7 \pm 1.4$	$307.6 \pm 0.2$	$123.0 \pm 0.4$	124.6
	18.8	$12.7 \pm 0.6$	$307.82 \pm 0.04$	$125.1 \pm 0.2$	
12	11.8	$3.1 \pm 0.6$	$307.7 \pm 0.1$	$125.5 \pm 0.2$	125.4
	18.8	$7.4 \pm 0.3$	$307.84 \pm 0.03$	$125.74 \pm 0.06$	
13	11.8	$2.7 \pm 0.5$	$307.6 \pm 0.2$	$124.4 \pm 0.1$	124.4
	18.8	$5.9 \pm 0.3$	$307.79 \pm 0.04$	$124.58 \pm 0.07$	

<sup>a</sup> The values of  ${}^1J_{\text{CH}_i}$  obtained from the spectrum of 5CB in  $\text{CDCl}_3$  are shown in the last column for comparison with values of  $c_i$ .

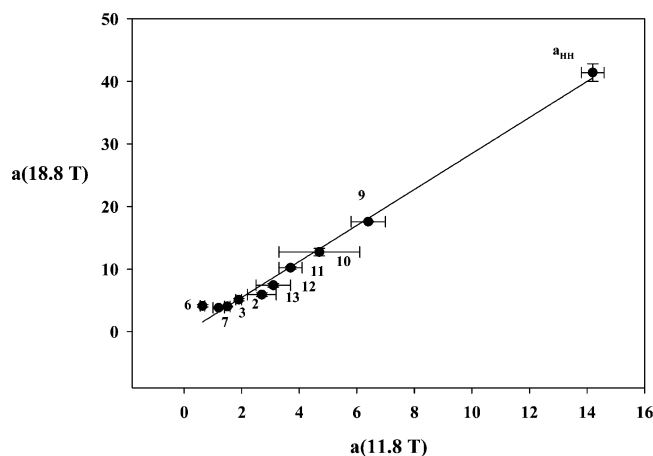
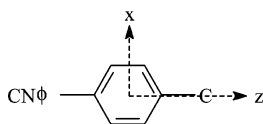


**Figure 10.** Ratio of  $a_i$  values obtained from the temperature dependences of  $D_{\text{HH}}^{\text{B}}$  and  ${}^1\Delta_{\text{CH}_i}$  (labeled with the position  $i$ ) at values of  $B_0$  of 11.75 and 18.79 T.

frame is described by the Wigner matrix  $D_{p,m}^2(\Omega_j^r)$ . For 5CB the rigid fragments, and their interaction tensor contributions,  $\epsilon_{2,p}(j)$ , are chosen to be the following:

$$\epsilon_{zz} \text{ and } \epsilon_{xx} - \epsilon_{yy} \text{ for}$$



$\epsilon_{\text{CC}}$  for a C–C bond in the aliphatic chain;

$\epsilon_{\text{CH}}$  for a C–H bond in the aliphatic chain.

The structure and orientation relative to the reference axes  $xyz$  of the cyanylated ring affect the values derived for  $\epsilon_{zz}$  and  $\epsilon_{xx} - \epsilon_{yy}$ , but they do not need to be taken into account explicitly. This is a consequence of the  $C_{2v}$  symmetry of the inter-ring bond rotation potential.

The potential energy for rotation about each of the chain  $\text{C}_r\text{--C}_{r+1}$  bonds, through an angle  $\phi_r$ , with  $r = 9\text{--}11$  is assumed to have minima at  $\phi_r = 0^\circ$  (trans), and  $\pm 112^\circ$  ( $\pm$ gauche), with

an energy difference  $E_{\text{tg}}$  and conformers with other values of  $\phi_r$  are neglected. Rotation about the C8–C9 bond is taken to have 2-fold symmetry with minima at  $\phi_8 = 90^\circ$  and  $270^\circ$ , which correspond to the plane C8–C9–C10 being orthogonal to the attached ring plane.<sup>15</sup> Only these two conformations of ring and chain are considered to be populated. The bond lengths and angles are chosen to be those used previously for the study of 5CB in the nematic phase.<sup>14</sup>

The mean internal energy,  $U_{\text{int}}(n)$  is assumed to have the form

$$U_{\text{int}}(n) = N_g(n)E_{\text{tg}} + \sum_{i < j} (E_i E_j)^{1/2} ((A_i + A_j)/r_{ij})^{12} \quad (30)$$

where  $N_g(n)$  is the number of gauche configurations in conformer  $n$ . The summation in eq 30 was taken only over hydrogen atoms, and only those which are separated by four or more bonds. The parameters  $E_i$  and  $A_i$  are given the values optimized to fit the data for 5CB in the nematic phase ( $E_{\text{H}} = 0.15 \text{ kJ mol}^{-1}$ ,  $A_{\text{H}} = 0.85 \text{ \AA}$ ), which give a significant contribution to  $U_{\text{int}}(n)$  only for severely sterically hindered conformers.

The data set used for the nematic phase was the quadrupolar splittings,  $\Delta\nu_i$ , obtained for a sample deuterated in each chain position, and in the attached phenyl ring. The mean ring quadrupolar splitting,  ${}^{1/2}(\Delta\nu_6 + \Delta\nu_7)$ , and the five quadrupolar splittings for the alkyl chain deuterium nuclei were used to obtain a common value of  $E_{\text{tg}} = 3.28 \text{ kJ mol}^{-1}$  for each bond rotation in the alkyl chain. A similar data set for the pre-transitional region at  $T - T_{\text{NI}} = 0.2 \text{ }^\circ\text{C}$  was chosen as the mean of the ring dipolar couplings,  ${}^1D_{\text{CHring}}^{\text{B}} = (1/2)({}^1D_{\text{CH}_6}^{\text{B}} + {}^1D_{\text{CH}_7}^{\text{B}})$ , plus the five values of  ${}^1D_{\text{CH}_i}^{\text{B}}$  for the alkyl chain, and these were matched to values calculated by varying  $\epsilon_{zz}$ ,  $\epsilon_{xx} - \epsilon_{yy}$ ,  $\epsilon_{\text{CC}}$ , and  $\epsilon_{\text{CH}}$ , with  $E_{\text{tg}}$  fixed at  $3.28 \text{ kJ mol}^{-1}$ . The calculated and observed values of  ${}^1D_{\text{CH}_i}^{\text{B}}$  are given in Table 5.

The agreement is excellent, which is strong support for the method used to derive conformational distributions and orientational order in both liquid crystalline and isotropic phases. Note too, that, as expected, for the isotropic phase  $P(n, T = 308.6 \text{ K}) = P_{\text{iso}}(n, T = 308.6 \text{ K})$ . A similarly good agreement between

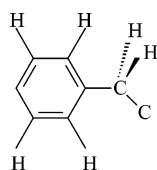
**TABLE 5: Observed Values of  ${}^1D_{\text{CH}i}^{\text{B}}$  at  $T - T_{\text{NI}} = 0.2$  °C Compared with Those Calculated Using the AP Method with  $E_{\text{lg}}$  Fixed at  $3.28 \text{ kJ mol}^{-1}$**

position	${}^1D_{\text{CH}i}^{\text{B}}/\text{Hz}$	
	observed	calculated
ring	$2.58 \pm 0.05$	2.57
9	$11.75 \pm 0.05$	11.80
10	$7.36 \pm 0.05$	7.14
11	$7.90 \pm 0.05$	7.86
12	$4.85 \pm 0.05$	5.11
13	$3.60 \pm 0.05$	3.50

observed and calculated values of  ${}^1D_{\text{CH}i}^{\text{B}}$  is obtained for temperatures up to  $T - T_{\text{NI}} = 1.4$  °C.

The calculated value of  $D_{\text{HH}9}^{\text{B}}$  for 308.6 K is 0.77 of that observed, and a similar difference holds for other temperatures. Including this coupling in the fitting process for the pre-transition data, while keeping the same geometrical parameters as used for the nematic phase does not change appreciably the agreement between observed and calculated values of the  ${}^1D_{\text{CH}i}^{\text{B}}$ , and so does not change the conclusion that the  ${}^{13}\text{C}-\text{H}$  couplings observed in the isotropic phase provide strong support for the method used to derive conformational distributions and orientational order in both liquid crystalline and isotropic phases.

It is interesting to speculate on why the observed and calculated values of the  $D_{\text{HH}9}^{\text{B}}$  are in poor agreement. The most probable reason is that the geometry of the fragment requires



adjustment. However, including  $D_{\text{HH}9}^{\text{B}}$  into the data set used to obtain the structure (and hence of the conformational distribution) raises the problem of the effect on dipolar and quadrupolar couplings of vibrational motion. The model being tested here for obtaining the conformational distribution uses quadrupolar splittings for the nematic phase, and C–H dipolar couplings for the isotropic phase. The dipolar couplings are related to  $\bar{C}_{\text{CH}i}$ , the average over all conformations of the order parameter for the  $\text{C}_i-\text{H}$  bond (cf eq 15):

$${}^1D_{\text{CH}i} = -K_{\text{CH}} \bar{C}_{\text{CH}i} \quad (31)$$

The quadrupolar splitting for the same site,  $\Delta\nu_i$ , is related to  $\bar{C}_{\text{CD}i}$ , which is assumed to equal  $\bar{C}_{\text{CH}i}$ , and also to  $\bar{C}_{\text{CD}i}^{\text{biaxial}}$ , a biaxial order parameter, averaged over all conformations, of axes orthogonal to the bond direction, by

$$\Delta\nu_i = \frac{3}{2} \bar{C}_{\text{CD}i} q_{\text{CD}i} + \left(\frac{3}{2}\right)^{1/2} \bar{C}_{\text{CD}i}^{\text{biaxial}} \Delta q_{\text{CD}i} \quad (32)$$

where  $q_{\text{CD}i}$  is the component along the C–D bond of the deuterium quadrupolar tensor, and  $\Delta q_{\text{CD}i}$  is the difference in components orthogonal to the bond. The second term in eq 32 is usually much smaller than the first and is often neglected, as was the case when analyzing the quadrupolar splittings observed for 5CB in the nematic phase.<sup>13,14</sup> In this case, the simple result is obtained that both  ${}^1D_{\text{CH}i}^{\text{B}}$  and  $\Delta\nu_{\text{CD}i}$  are directly proportional to  $\bar{C}_{\text{CH}i}$  and can be considered to be equivalent data sets. This conclusion also assumes that both  ${}^1D_{\text{CH}i}^{\text{B}}$  and  $\Delta\nu_{\text{CD}i}$  are affected in a similar way by vibrational averaging. This assumption has not been tested, but it can be argued to be reasonable since for

both interactions the largest effect of vibrational motion in each conformer of the molecule will be to average the orientation of the C–H or C–D bond relative to the principal axes of the order matrix of that conformer. The effect of vibrational motion on  $D_{\text{HH}9}^{\text{B}}$  is probably of a different magnitude from that on the C–H couplings, since now the dominant effect will come from low-frequency modes which change both the orientation and magnitude of the vector  $\mathbf{r}_{\text{HH}}$ .

## Conclusions

The advantages of using NMR spectroscopy to study pre-transitional ordering was first demonstrated using deuterium as the resonant nucleus.<sup>4,5</sup> In contrast to the “classical” experiments, the NMR experiments can explore the effects of molecular symmetry and flexibility. However, the need to deuterate the mesogenic molecules has severely limited the application of this method. It is clear from this study on 5CB that using  ${}^{13}\text{C}$  and  ${}^1\text{H}$  as the resonant nuclei gives the same information as deuterium on pre-transitional ordering of molecules, but without the need of isotope enrichment, and so the method can be applied in principle to any liquid crystalline sample.

The values of  $D_{ij}^{\text{B}}$  obtained from these experiments can be used to test predictions for the temperature dependence of these couplings, and most importantly the data at temperatures close to  $T_{\text{NI}}$  may be used to derive the conformational distribution of the mesogenic molecules in the isotropic phase. The data analyzed here for 5CB show that  $P_{\text{iso}}(n, T)$  obtained from quadrupolar splittings in the nematic phase is virtually identical with  $P(n, T)$  obtained from magnetic field induced C–H dipolar couplings in the isotropic phase. This gives strong support to the theoretical models used to analyze data obtained on liquid crystalline phases which yield  $P(n, T)$ , and predict  $P_{\text{iso}}(n, T)$ .

The present study has been on a representative nematogen, but the NMR experiments demonstrated here can be applied to any liquid crystalline sample. In particular, it will be very interesting to extend these studies of field induced dipolar couplings to mesogens which have a high degree of molecular flexibility such that in the liquid crystalline phase there is predicted to be a very large difference between  $P(n, T)$  and  $P_{\text{iso}}(n, T)$ , this work is currently underway.

The magnitude of the field induced couplings depend on  $\mathbf{B}_0^2$ , and although it is obviously an advantage to use a spectrometer operating at the very highest fields available (at the moment this corresponds to static fields of  $\sim 21$  T), useful data can also be obtained at lower fields, such as 11.75 T for the 5CB compound.

**Acknowledgment.** The experiments at 800 MHz were done on the spectrometer at the Institut de Biologie Structurale in Grenoble. We are very grateful to Dr. Martin Blackledge for arranging for our first experiments done there and to Dr. Adrien Flavir for technical assistance.

## References and Notes

- (1) Luckhurst, G. R. *J. Chem. Soc., Faraday Trans.* **1988**, *84*, 961.
- (2) de Gennes, P. G. *Physics of Liquid Crystals*; Clarendon Press: Oxford, 1974.
- (3) Lohman, J. A. B.; MacLean, C. *Chem. Phys.* **1978**, *35*, 269.
- (4) Attard, G. S.; Beckmann, P. A.; Emsley, J. W.; Luckhurst, G. R.; Turner, D. L. *Mol. Phys.* **1982**, *45*, 1125.
- (5) Attard, G. S.; Emsley, J. W.; Khoo, S. K.; Luckhurst, G. R. *Chem. Phys. Lett.* **1984**, *105*, 244.
- (6) Facke, T.; Berger, S. *J. Magn. Reson. Ser. A* **1995**, *113*, 114. Farjon, J.; Merlet, D.; Lesot, P.; Courtieu, J. *J. Magn. Reson.* **2002**, *158*, 169.



- (7) Geen, H.; Freeman, R. *J. Magn. Reson.* **1991**, *1*, 93.
- (8) Bax, A.; Freeman, R.; Frenkiel, T. A. *J. Am. Chem. Soc.* **1981**, *103*, 2102.
- (9) Heaton, N. J. Ph.D. Thesis, University of Southampton, 1986.
- (10) Heaton, N. J.; Luckhurst, G. R. *Mol. Phys.* **1989**, *66*, 65.
- (11) Brink, D. M.; Satchler, G. R. *Angular Momentum*, 2nd ed.; Clarendon Press: Oxford, 1975; p 54.
- (12) Coles, H. J.; Jennings, B. R. *Mol. Phys.* **1978**, *36*, 1661.
- (13) Emsley, J. W.; Luckhurst, G. R.; Stockley, C. P. *Proc. R. Soc. London* **1982**, *A381*, 117.
- (14) Emsley, J. W.; Lesot, P.; Courtieu, J.; Merlet, D. *Phys. Chem. Chem. Phys.* **2004**, *6*, 5331.
- (15) Emsley, J. W.; De Luca, G.; Celebre, G.; Longeri, M. *Liquid Cryst.* **1996**, *20*, 569.